ANOMALOUSLY EARLY ONSET OF SPRING IN THE CESM LARGE ENSEMBLE

Honors Thesis

Presented to the College of Agriculture and Life Sciences, Physical Sciences

of Cornell University

in Partial Fulfillment of the Requirements for the

Research Honors Program

by

Zachary M. Labe

May 2015

Professor Toby R. Ault

Abstract

Identifying seasonal transition remains a source of great uncertainty in climate prediction albeit their potentially significant impacts to a wide variety of natural and physical systems. While the effects of anomalously early season warmth across North America are widely documented, their frequency and predictability under climate change remain unclear. The following study utilizes the Extended Spring Indices model to classify the onset of spring through a variety of gridded observational and model data sets. Using the new 1°x 1°Community Earth System Model Large Ensemble project, this study documents the frequency, magnitude, and mechanisms for early spring onset through historical and future simulations. The threshold for extreme early season warmth is established by the record breaking spring in March 2012. The primary geographic region for the analysis is across the central and northern United States. While these events are nearly statistically random in historical observations, the modeled results indicate a significantly increased frequency and earlier timing of spring during the 21^{st} century as a result of both internal climate variability and climate change. In addition, the long wave patterns during these synoptic warm events reveal notable similarities in jet dynamics and structure. These findings suggest early spring onset may have further temporal predictability despite the influence of climate change.

Acknowledgments

I would like to acknowledge the support and guidance of my research advisor, Dr. Toby Ault, whose mentoring and resources led to the success of this project. Additionally, I would like to thank Mark Wysocki for his continued words of encouragement during my undergraduate career. I am also grateful for the assistance from Richard Moore for all things Python. Grant support for this project is in part by the USA National Phenology Network and United States Geological Survey through employment of the SI-x models and phenological data. The original SI-x code was developed by Dr. Mark D. Schwartz of the University of Wisconsin-Milwaukee, and the CESM1(CAM5) Large Ensemble Community Project and supercomputing resources were provided by NSF/CISL/Yellowstone.

Contents

List of Tables

List of Figures

1 Introduction

Widespread early season warmth during March of 2012 led to the second largest areal size of above normal temperatures for any March on record across the United States (Karl et al., 2012). The magnitude of warmth led to the warmest March in historical records with over 15,000 warm records broken across the continental United States (Blunden and Arndt, 2013). The greatest positive temperature departures occurred across the Midwest and Great Lakes. In fact, Chicago, IL alone recorded nine consecutive days breaking or tying high temperature records and an overall +15.6°F mean temperature departure for the entire month (US Department of Commerce, NOAA, 2012). The summer-like temperatures resulted in a sudden bloom of agricultural crops, fruit trees, and other plants. Phenological metrics reported March 2012 as the earliest ecological spring since 1900 (Ault et al., 2013). As temperatures returned to their climatological averages by early April, plants and crop yields faced a significantly higher threat from frosts and freezes. Severe economic losses occurred across a large expanse of the Midwest and Northeast as a response to the early season warmth. Michigan alone reported nearly $500 million in agricultural damages (Knudson, 2012).

Dole et al. (2014) documents the favorable conditions that led to the anomalously early spring in which significant warm air advection transported heat northward across the center of the country in response to a large anticyclone across the Great Lakes. Upper air analysis indicates a deep trough axis across the eastern Pacific Ocean and western United States with increasing ridge amplification toward the east. This trough-ridge structure propagation is likely the result of an enhanced MJO event during the end of February (Dole et al., 2014). This pattern is also characteristic of other early spring seasons across the same regions of the United States (Ault et al., 2013; Dole et al., 2014).

Acknowledging the significance of these early warm synoptic events is critical given the influences of natural and anthropogenic climate variability and forcing expected over at least the next century (IPCC, 2014). Classification of the timing of these events is often difficult to determine given the myriad of variables during transition seasons. However, phenological events have demonstrated to be a remarkably consistent spatial and temporal metric for both ecological and climate systems (Schwartz et al., 2012; Ault et al., 2013). While the USA National Phenology Network was only established in 2007 (data available at `https://www.usanpn.org/results/data`), phenology records for indicator species have been documented since the 1950s (Schwartz et al., 2012). Volunteers across a variety of climate zones send in their reports for several species of plants in regards to their timing of the first leaves and blooms. Optimizing phenological and climatological data over an extended period during the 20th century allowed for the development of the original spring indices model (Schwartz, 1993) requiring only the meteorological inputs of surface temperature. In return, the model produces an output regarding the onset of spring as a "day of year" *(DOY, i.e. Jan. 1st=1)* for several metrics.

Globally, increased surface warming in response to climate change will likely present noticeable changes in the transition periods between seasons. In particular, the frequency and development of anomalous warm synoptic events during early spring are relatively undocumented. However, a new climate model ensemble simulation from the National Center for Atmospheric Research (NCAR) provides a source of understanding the winter to spring transition period under climate change and internal variability. Furthermore, this study focuses on extreme early springs across the United States and their potential predictability through the 21st century. The phenological model of the spring indices provides a declarative classification of spring that is applicable for a variety of climate zones, and therefore is utilized throughout the project. Assessing the relative occurrence and development of these extreme events may provide critical for determining the effects of climate change on the atmosphere and biosphere.

2 Methods

To classify the onset of spring, the extended spring indices (SI-x) were computed for a variety of gridded data sets (Schwartz et al., 2006a, 2013; Ault et al., 2014b). The SI-x are phenological models, which use lilac and honeysuckle as proxies to denote atmospheric and ecological changes in the transition period from winter to spring across a variety of spatial scales (Schwartz, 1994). Phenological data has been widely collected since the early 20th century by selected observers and now has expanded through satellite and public volunteering (van Vliet et al., 2003). The SI-x provide a method of classifying the timing of spring that is standard across a variety of geographic and climate zones in North America.

The SI-x code is documented online in its entirety ((Ault et al., 2014b) available at `http://ecrl.eas.cornell.edu/Misc/Publications/Ault_si-ml_v5.0.1.pdf`); however, its inputs are simply daily T_{max} and T_{min} for a given latitude. Three function outputs are produced including: first leaf, first bloom, and last freeze. For the purposes of this analysis,"first leaf" was selected as the primary metric to characterize the onset of spring given the large temporal scale of the model simulations. The three metric outputs are denoted as a particular day of the year since January 1st (*DOY=1*). Phenological coefficients have been calculated to account for lilac and honeysuckle in addition to a formula for the computation of "high energy synoptic events" given the inputs of T_{max} and T_{min} (Schwartz, 1985; Ault et al., 2014b). The synoptic events counter is used to denote changes in atmospheric dynamics that may be responsible for early season warmth. In addition, growing degree hours and daylight are also calculated.

To characterize anomalously early springs in the LENS, March 2012 was selected as a benchmark given its nearly -3σ first leaf and bloom onset. Thirty year climatological averages for SI-x were first calculated utilizing daily surface temperature data from the new 1°x 1°gridded Berkeley Earth Surface Temperature (BEST) project (Mueller, 2013) over the period from 1981-2010. This temperature network is derived from from the Global Historical Climate Network (GHCN) and other temperature records. A variety of statistical methods are then applied to each grid. March 2012 SI-x anomalies are greatest across the upper Great Lakes and particularly around portions of Wisconsin, Minnesota, and the upper peninsula of Michigan (Dole et al., 2014). This general geographic region (37.5°N to 50.5°N and -101.5°W to -75.5°W) was restricted for all further calculations in observational and modeled analysis **(Figure 2)**.

To understand the occurrences and synoptic patterns resulting from early spring onset, it is critical to analyze the natural and anthropogenic forcing of climate change. The National Center for Atmospheric Research's Community Earth System Model Large Ensemble (LENS) project was developed to analyze and resolve internal climate variability for pre-industrial and post-industrial simulations of Earth (Kay et al., 2014). A 1000 year control rule was spun up without the influences of anthropogenic climate change based on the Community Atmosphere Model version 5 CESM1(CAM5) fully coupled land and atmosphere model, which assumed 1850 land, ocean, and atmosphere forcings (Kay et al., 2014). At the start of January 1, 1920 thirty ensembles were initialized using the same initial conditions and spread dictated by only a small temperature round-off error (Kay et al., 2014). The ensembles were run from 1920 through 2005 representing the historical forcing of the post-industrialization era for greenhouse gases and temperature rises. During the period from 2006 to 2100, the ensembles were forced using the Representative Concentration Pathway 8.5 (RCP8.5) to account for modeled 21st century global warming with average global surface temperature increases of around 5 Kelvin in the ensembles by the end of the simulation (Kay et al., 2014).

Pearson correlation coefficients were calculated through the CESM control run beginning at year 402 through 999 to locate spatial patterns similar to March 2012. The nine closest matches to 2012 were highlighted for further analysis through SI-x anomalies and synoptic weather variables. Furthermore, early spring onset frequency was analyzed through the LENS historical period (1920-2005) by denoting anomalous thresholds of -2σ and -3σ using detrended z-scores. Lastly, the future period (2006-2100) in the LENS project was analyzed for the same early spring onset thresholds with z-scores calculated using the previous historical climatological average first leaf and standard deviation as references. The historical and future ensembles were analyzed over the previously designated geographic region across the central United States. A variety of teleconnection and synoptic weather variable outputs are available via the LENS project and were analyzed for pattern similarities that result in early season warmth across the contiguous United States and southern Canada. For this project, sea level pressure, 200 mb and 500 mb u/v winds, and 2m surface temperatures were selected for comparisons.

3 Results and Discussion

Average SI-x values using the BEST gridded data network are plotted for central North America over the 1981-2010 climatological period **(Figure 1)**. Indices are generally altitude and latitudinal dependent across the United States for both leaf and bloom dates (Ault et al., 2014a) as a result of spring jet dynamics and day length. Anomalies for March 2012 were calculated by subtracting the leaf and bloom index values from the climatological mean per grid point **(Figure 2)**. The greatest anomalies are located over the Great Lakes and upper Midwest for the leaf index values with leaf out occurring nearly 40 days earlier than normal in this region. It should also be noted that SI-x dates across the Pacific northwest averaged later than normal. This suggests regional differences in SI-x onset are likely a result of long waves and large-scale teleconnection patterns (Ault et al., 2013). Plotted NCEP-DOE Reanalysis II (Kanamitsu et al., 2002) sea level pressure patterns indicate exceptional ridging over the center of the country with a low pressure axis located near the Gulf of Alaska. This setup is consistent with a strong poleward transport of heat as warm air advection increased daily temperature departures to nearly 50°F above normal during the height of the warmth in March 2012 across the upper Midwest. The southerly flow and geopotential height patterns are likely a result of an enhanced MJO-driven wave ($+2\sigma$) that propagated eastward during the middle to end of February across the equatorial Pacific (Dole et al., 2014).

In comparison, Dole et al. (2014) also suggests similar dynamics were evident in March 1910 during an anomalously early spring again across the Great Lakes as a result of strong warm air advection out of the southwest in response to an anomalous jet transporting heat northward (Compo et al., 2011). While the SI-x for March 1910 are approximately only around -2σ, the overall synoptic wavelengths across North America remain quite similar to March 2012 as evidence through their daily mean 200mb wind and height fields **(Figure 3)**. These pattern features are further noted during the following discussion of early springs in the LENS project.

A simple linear regression was calculated over the entire 1880-2013 BEST gridded data set for the previously defined geographic region across the Midwest and Great Lakes. Leaf and bloom out values are occurring approximately 0.5 days/decade earlier than normal over the period with March 2012 having the largest anomaly **(Figure 4)**. However, during the 1981-2010 climatological period this trend increases to nearly 1 days/decade earlier. First leaf and bloom indices are plotted and detrended to compute z-scores. Both leaf and bloom z-scores for March 2012 compute to approximately -3σ.

3.1 CESM Pre-Industrial Control

SI-x were calculated from daily T_{max} and T_{min} over the CESM control simulation. The control run assumes internal climate variability without the influences of anthropogenic forcings (Kay et al., 2014). Select years for analysis began with the arbitrary NCAR model selected date of January 1st, year 402 and lasted through December 31st, year 999. Given expected model noise and internal climate variability, SI-x assume no changes in spring onset trends through the simulation. To understand the frequency, magnitude, and dynamics of anomalously early spring onset in the absence of climate change, Pearson correlation coefficients were calculated between each year to identify 2012-like patterns **(Figure 5)**. The nine closest matches for leaf and bloom indices were plotted assuming January 1st as day one **(Figures 6 and 8)**. Additionally, leaf and bloom index anomalies were plotted for the same CESM year matches **(Figures 7 and 9)**. Individual years were subtracted from the average SI-x dates as calculated over the entire control simulation. As a result of the greatest synoptic pattern signal from leaf onset dates, the leaf index values primarily will be used for continued analysis.

Restricting the geographic domain to the Midwest and Great Lakes (37.5°N to 50.5°N and -101.5°W to -75.5°W), leaf index values (DOY) were plotted through the control run. A negative three standard deviation threshold was placed on the values for a comparison with March 2012. Z-scores were calculated for each year using the mean and standard deviation from the control as reference for this period of natural climate variability. Only two years resulted in leaf index dates above the 2012 threshold: 406 and 653. The outlier year 653 had an approximately -4.5σ early leaf index with spring occurring nearly 40 days earlier than normal across the Midwest **(Figure 7)**. An area of later than normal leaf out is denoted across parts of the Southwest. Most of the CESM control's closest corresponding patterns contain this dipole pattern, which has also been previously documented in historical climatologies of trends in spring onset (Schwartz et al., 2013; Ault et al., 2014a). Assuming the limited early spring onset threshold years through the entire control simulation, their occurrence is nearly random; however, a -2σ spring onset is expected roughly twice per century.

Further analysis of year 653 suggests a series of high amplitude waves propagated across the Pacific Ocean eastward into the contiguous United States during the two weeks near the leaf out period. A large but diminishing Aleutian low is evident south of Alaska and an anticyclone over southern Canada and the northeastern United States **(Figure 11)**. This pattern is not at all dissimilar to that noted in March 2012 and even 1910. Plotting 200mb wind vectors and contoured magnitude values **(Figure 12)** suggest jet dynamics may play a critical role in the transfer of heat northward in response to an unusually strong jet streak out of the eastern Pacific and into the southwestern United Sates. Furthermore, this interpretation is similar to the pattern responsible for March 2012 **(Figure 3)**. Daily temperature climatologies were also calculated per one hundred years given the expected noise in the 1850 pre-industrialization forcing on the CESM control. All nine CESM matches contained significantly positive temperature departures across the central and eastern United States in association with strong warm air advection **(Figure 13)** with a similar spatial pattern as March 2012.

3.2 LENS 20$^{\text{th}}$ Century Historical

Through NCAR's LENS project, 30 ensembles runs were initialized from an arbitrary date in the control and induced a historical forcing from 1920-2005. Kay et al. (2014) documents that spread in the ensembles was applied through a small round-off error in their initial temperature fields. The ocean state remained identical for each member.

To investigate the frequency of early spring onset in the "historical" period from the LENS, z-scores were first calculated for each member and for each year in their associated run. Z-scores were detrended and further normalized using the CESM control mean leaf index and standard deviation. The mean trend for all ensembles members is approximately 0.23 days/decade earlier, nevertheless some member variability is evident. This is also slightly less than the trend in the gridded BEST data set **(Figure 4)**. The CMIP5 historical runs and other climate models routinely have difficulty resolving detectable anthropogenic warming trends particularly across the midlatitudes, and this suggests one possible difference in the expected observed and modeled surface warming trends for earlier spring onset (Knutson et al., 2013).

Each ensemble projection was plotted for frequency of early spring onset thresholds of -2σ and -3σ **(Figure 14)**. Excluding expected model noise, the results are relatively consistent with the pre-industrial forced control run. Moreover, we see no increased frequency in earlier than normal springs across the central United States through the simulated historical period despite a gradual warming trend globally. At the same time, It is also important to note that global long-term temperature trends in the LENS fall within the lower range of spread in expected land temperature increases (Kay et al., 2014).

Upper air analysis of the -3σ years is consistent with our expected high amplitude long wave pattern. Peak warmth periods in the Midwest are consistent with a trough axis along the eastern Pacific and an anomalous jet streak out of the southwestern United States. Strong poleward transport of heat is indicated in both events north through south-central Canada. In contrast, one of the two years orients the core of the earliest leaf index anomalies farther west across the central Rockies and extending eastward through the Great Lakes. As a result, we do not see the dipole SI-x dates structure closely associated with other anomalously early springs. Interpretations of these results are again limited by the near random occurrence of these significant warm air advection events and potential ensemble noise through its handling of internal climate variability.

3.3 RCP8.5 Forced Future Ensembles

Applying RCP8.5 forcing through an A2 IPCC emissions scenario, the thirty ensembles members were extrapolated through 2100 (Lamarque et al., 2011). All members increased global surface temperatures by around 5 Kelvin through global warming by year 2100 (Kay et al., 2014). To reveal the effects of increased boundary layer warmth and climate change on spring onset, each ensemble member's (2006-2080) daily T_{max} and T_{min} were applied to the SI-x model. Z-scores were calculated using the LENS historical period as reference. Results were further detrended to account for a mean ensemble trend of spring onset occurring 2.6 days/decade earlier **(Table 1)**. The same defined geographic region across the north central United States **(Figure 2)** was used for this analysis.

Results support a remarkable increase in both the frequency and magnitude of early spring onset across this region through the 21st century **(Figure 15)**. Strong agreement between each ensemble member supports of a frequency of -3σ leaf out years at roughly 20.8 per temporal period. Importantly, we see multiple ensemble occurrences of -4σ and -5σ springs per each run with the earliest leaf date out of all members at approximately day 66. Most ensembles have a minimum of around day 72, which is exceptionally earlier than March 2012 or other simulations in the control or historical ensembles.

4 Conclusions

Understanding the dynamic pattern transitions from winter to spring across the midlatitudes is of critical importance in respect to natural and anthropogenically forced climate change. As a result of internal climate variability and regionally-based trends, classifying and discerning seasonal progression has been a significant challenge for climate prediction The extended spring indices (SI-x) provide a statistical phenological model to classify the onset of spring and have been expanded to provide a standard proxy through space and time (Schwartz, 1985; Schwartz et al., 2006b, 2013; Ault et al., 2014b). The SI-x model requires inputs of daily T_{max} and T_{min} and a given latitude to produce three output parameters based on the indicator species of lilac and honeysuckle: first leaf, first bloom, and last freeze. Limitations of the model include no input variables for precipitation, snow cover, or soil moisture; additionally, synoptic events are only calculated based on the surface temperature inputs (Ault et al., 2014b).

The consequences of the anomalous warmth and ecological bloom in March of 2012 proved costly for agricultural and energy demands across the northern latitudes of the United States. The SI-x model regarded March 2012 as the earliest spring on record since 1900 with leaf and bloom values occurring nearly 40 days earlier than normal (Ault et al., 2013). As temperatures returned closer to climatological normals by early April, crops were substantially more vulnerable to frost and freezes. Estimated agricultural losses totaled nearly half a billion dollars in Michigan (Knudson, 2012).

To understand the frequency and dynamics of anomalously early springs in a warming global climate (IPCC, 2014), several sets of observed and modeled data were analyzed using the SI-x model. Climatologies since 1880 were analyzed using the new gridded Berkeley Earth Surface Temperature project that employs a combination of historical observations and statistical methods to resolve daily surface temperatures on 1°x 1°grids (Mueller, 2013). Moreover, investigation of early spring onset was derived via NCAR's new Community Earth System Large Ensemble (LENS) project (Kay et al., 2014). The LENS is a 1°x 1°dynamic climate model based on the CAM5 and RCP8.5 forcing (data available `http://www.earthsystemgrid.org`). A control run was spun up for several hundred years before thirty ensembles differing in initial conditions by only a small temperature round-off error were run through 2100. Analyzing the CESM control simulation provides an atmosphere subject to internal climate variability and pre-industrial (1850) forcing. The LENS members impart historical 20st century runs (1920-2005), which is then further extended through 2100 as a result of increased anthropogenic forcing.

Anomalous early spring onset is defined by a minimum threshold of -3σ for purposes in comparison with March 2012. Historical climate records since 1880, confirmed by the BEST gridded data set, suggest such early springs are infrequent and an outlier. Furthermore, the CESM pre-industrial era control supports this result with a frequency of early springs at roughly once per century or less. Analyzing the LENS thirty members during the 1920-2005 also confirms this frequency and perhaps is only a result of random model noise and variability. Exploring the synoptic and long wave patterns responsible for earlier springs through NCEP-DOE Reanalysis II (Kanamitsu et al., 2002) and LENS output poses a potentially important composite. All of the early spring dates in the previously mentioned data sets were defined by a set of correspondingly similar atmospheric dynamic patterns. Exceptional early season warmth across the region was often in direct response to a high amplitude trough in the eastern Pacific and ridge across the central to eastern continental United Sates resulting in an anomalous poleward transport of heat as indicated by 200mb, 500mb, and 850mb vector composites. A strong jet streak was often noted moving into western California and eventually the Southwest. Similarly, a low pressure axis south of Alaska implies a southern shift and weakening of the Aleutian Low, which is fairly common in negative Pacific Decadal Oscillations (PDO). The influences of the PDO and spring onset of been widely explored (Ault et al., 2014a), particularly across the Pacific Northwest where -PDO regimes are often responsible for later springs (McCabe et al., 2013). This is consistent with later SI-x dates for western locations during periods of anomalous warmth farther east. These patterns are exhibited in most all modeled and observed case studies.

Advancing the LENS members through 2100 under RCP8.5 forcing reveals a striking result in regards to both frequency and magnitude of the early spring onset threshold. The prevalence of such springs increases to approximately 20.8 years per member run from 2006-2080. Likewise, an increase in magnitude of early springs is also noted through all scenarios including an anomaly of -5.88σ for one year (leaf out at day 66). Trends in earlier springs over the period increase significantly with a mean onset occurring at nearly 2.6 days/decade earlier. Kay et al. (2014) documents that all thirty ensemble members are subjected to global surface warming by nearly 5 Kelvin. Therefore, this outcome suggests the timing of spring is likely directly related to an overall trend in increasing surface temperatures. Moreover, it is likely these anomalous patterns have a potential temporal predictability given the similarities in high amplitude long wave patterns among documented and modeled events.

4.1 Future Work

Continued development of this project will entail analyzing the LENS (2006-2080) members and their particular synoptic and teleconnection environments resulting in early season warmth, particularly for years of greatest magnitude anomaly. The regional trends in spring onset in response to teleconnection climate modes have been widely documented (McCabe et al., 2011, 2013; Schwartz et al., 2013; Ault et al., 2014a); however, progress is needed to interpret these scales under climate change and their corresponding relation to the timing of spring during the 21^{st} century. The Climate Variability Diagnostics Package (CVDP) imparts further data concerning these indices through the LENS simulation (Phillips et al., 2014). Additional evidence is also needed to understand the trough and ridge structure that is common among early spring onset events. Interpreting these variables may lead to an eventual statistical model for potential predictability in anomalously early spring onset, which will assist in a wide variety of public industries ranging from agricultural to energy.

References

Ault, T. R., G. M. Henebry, K. M. de Beurs, M. D. Schwartz, J. L. Betancourt, and D. Moore, 2013: The False Spring of 2012, Earliest in North American Record. *Eos, Transactions American Geophysical Union*, **94 (20)**, 181–182, doi:10.1002/2013EO200001, URL http://dx.doi.org/10.1002/2013EO200001.

Ault, T. R., M. D. Schwartz, and R. Zurita-milla, 2014a: Trends and natural variability of North American spring onset as evaluated by a new gridded dataset of spring indices.

Ault, T. R., R. Zurita-Milla, and M. D. Schwartz, 2014b: A Matlab toolbox for calculating spring indices from daily meteorological data. *Computers & Geosciences (submitted).*

Blunden, J., and D. S. Arndt, 2013: State of the Climate in 2012. *Bulletin of the American Meteorological Society*, **94 (8)**, S1–S258, doi:10.1175/2013BAMSStateoftheClimate.1, URL http://journals.ametsoc.org/doi/abs/10.1175/2013BAMSStateoftheClimate.1.

Compo, G. P., and Coauthors, 2011: The Twentieth Century Reanalysis Project. *Quarterly Journal of the Royal Meteorological Society*, **137 (654)**, 1–28, doi:10.1002/qj.776, URL http://doi.wiley.com/10.1002/qj.776.

Dole, R., and Coauthors, 2014: The making of an extreme event: Putting the pieces together. *Bulletin of the American Meteorological Society*, **95 (3)**, 427–440, doi:10.1175/BAMS-D-12-00069.1.

IPCC, 2014: Summary for Policymakers. *Climate Change 2014: Impacts, Adaptation, and Vulnerability. Part A: Global and Sectoral Aspects. Contribution of Working Group II to the Fifth Assessment Report of the Intergovernmental Panel on Climate Change*, C. B. Field, V. R. Barros, D. J. Dokken, K. J. Mach, M. D. Mastrandrea, T. E. Bilir, M. Chatterjee, K. L. Ebi, Y. O. Estrada, R. C. Genova, B. Girma, E. S. Kissel, A. N. Levy, S. MacCracken, P. R. Mastrandrea, and L. L. White, Eds., Cambridge University Press, Cambridge, United Kingdom, and New York, NY, USA, 1–32.

Kanamitsu, M., W. Ebisuzaki, J. Woollen, S.-K. Yang, J. J. Hnilo, M. Fiorino, and G. L. Potter, 2002: NCEPDOE AMIP-II Reanalysis (R-2). *Bulletin of the American Meteorological Society*, **83 (11)**, 1631–1643, doi:10.1175/BAMS-83-11-1631, URL http://journals.ametsoc.org/doi/abs/10.1175/BAMS-83-11-1631.

Karl, T. R., and Coauthors, 2012: U.S. temperature and drought: Recent anomalies and trends. *Eos, Transactions American Geophysical Union*, **93 (47)**, 473, doi:10.1029/2012EO470001, URL http://doi.wiley.com/10.1029/2012EO470001.

Kay, J. E., and Coauthors, 2014: The Community Earth System Model (CESM) Large Ensemble Project: A Community Resource for Studying Climate Change in the Presence of Internal Climate Variability. *Bulletin of the American Meteorological Society*, 141119125353005, doi:10.1175/BAMS-D-13-00255.1, URL http://journals.ametsoc.org/doi/abs/10.1175/BAMS-D-13-00255.1.

Knudson, W. A., 2012: The economic impact of this spring's weather on the fruit and vegetable sectors. *Strategic Marketing Institute, Michigan State University, Working Paper.*

Knutson, T. R., F. Zeng, and A. T. Wittenberg, 2013: Multimodel Assessment of Regional Surface Temperature Trends: CMIP3 and CMIP5 Twentieth-Century Simulations. *Journal of Climate*, **26 (22)**, 8709–8743, doi:10.1175/JCLI-D-12-00567.1, URL http://journals.ametsoc.org/doi/abs/10.1175/JCLI-D-12-00567.1.

Lamarque, J.-F., G. P. Kyle, M. Meinshausen, K. Riahi, S. J. Smith, D. P. van Vuuren, A. J. Conley, and F. Vitt, 2011: Global and regional evolution of short-lived radiatively-active gases and aerosols in the Representative Concentration Pathways. *Climatic Change*, **109 (1-2)**, 191–212, doi:10.1007/s10584-011-0155-0, URL http://link.springer.com/10.1007/s10584-011-0155-0.

McCabe, G. J., T. R. Ault, B. I. Cook, J. L. Betancourt, and M. D. Schwartz, 2011: Influences of the El Niño Southern Oscillation and the Pacific Decadal Oscillation on the timing of the North American spring. *International Journal of Climatology*, doi:10.1002/joc.3400, URL http://dx.doi.org/10.1002/joc.3400.

McCabe, G. J., J. L. Betancourt, G. T. Pederson, and M. D. Schwartz, 2013: Variability Common to First Leaf Dates and Snowpack in the Western Conterminous United States. *Earth Interactions*, **17 (26)**, 1–18, doi:10.1175/2013EI000549.1, URL http://journals.ametsoc.org/doi/abs/10.1175/2013EI000549.1.

Mueller, R., 2013: Berkeley Earth Temperature Averaging Process. *Geoinformatics & Geostatistics: An Overview*, doi:10.4172/2327-4581.1000103, URL http://www.scitechnol.com/2327-4581/2327-4581-1-103.php.

Phillips, A. S., C. Deser, and J. Fasullo, 2014: Evaluating Modes of Variability in Climate Models. *Eos, Transactions American Geophysical Union*, **95 (49)**, 453–455, doi:10.1002/2014EO490002, URL http://doi.wiley.com/10.1002/2014EO490002.

Schwartz, M. D., 1985: The advance of phenological spring across Eastern and Central North America. Ph.D. thesis, University of Kansas.

Schwartz, M. D., 1993: Assessing the Onset of Spring: A Climatological Perspective. *Physical Geography*, **14 (6)**, 536–550.

Schwartz, M. D., 1994: Monitoring Global Change with Phenology - the Case of the Spring Green Wave. *International Journal of Biometeorology*, **38 (1)**, 18–22.

Schwartz, M. D., R. Ahas, and A. Aasa, 2006a: Onset of spring starting earlier across the Northern Hemisphere. *Global Change Biology*, **12 (2)**, 343–351.

Schwartz, M. D., R. Ahas, and A. Aasa, 2006b: Onset of spring starting earlier across the Northern Hemisphere. *Global Change Biology*, **12 (2)**, 343–351, doi:10.1111/j.1365-2486.2005.01097.x, URL http://doi.wiley.com/10.1111/j.1365-2486.2005.01097.x.

Schwartz, M. D., T. R. Ault, and J. L. Betancourt, 2013: Spring onset variations and trends in the continental United States: past and regional assessment using temperature-based indices. *International Journal of Climatology*, **33 (13)**, 2917–2922, doi:10.1002/joc.3625, URL http://doi.wiley.com/10.1002/joc.3625.

Schwartz, M. D., J. L. Betancourt, and J. F. Weltzin, 2012: From Caprio's lilacs to the USA National Phenology Network. *Frontiers in Ecology and the Environment*, **10 (6)**, 324–327, doi:10.1890/110281, URL http://dx.doi.org/10.1890/110281.

US Department of Commerce, NOAA, N. W. S., 2012: March 2012: Unprecident Heat. URL http://www.crh.noaa.gov/news/display_cmsstory.php?wfo=lot&storyid=80740&source=2.

van Vliet, A. J. H., and Coauthors, 2003: The European phenology network. *International journal of biometeorology*, **47 (4)**, 202–12, doi:10.1007/s00484-003-0174-2, URL http://www.ncbi.nlm.nih.gov/pubmed/12734744.

Table 1: LENS RCP8.5 Trends 2006-2080 (days/decade)

Member	Leaf Index	Bloom Index
1	-2.5	-2.5
2	-2.9	-2.8
3	-2.5	-2.6
4	-2.5	-2.6
5	-2.5	-2.3
6	-2.7	-2.6
7	-2.5	-2.6
8	-2.3	-2.4
9	-2.5	-2.3
10	-2.0	-2.3
11	-1.8	-2.0
12	-2.5	-2.6
13	-2.5	-2.5
14	-2.6	-2.7
15	-2.6	-2.8
16	-2.3	-2.3
17	-3.3	-3.2
18	-3.3	-3.3
19	-3.0	-3.1
20	-2.6	-2.5
21	-2.4	-2.1
22	-2.5	-2.5
23	-3.0	-3.2
24	-2.7	-2.6
25	-2.8	-2.7
26	-2.8	-2.9
27	-2.8	-2.4
28	-2.4	-2.3
29	-3.1	-2.9

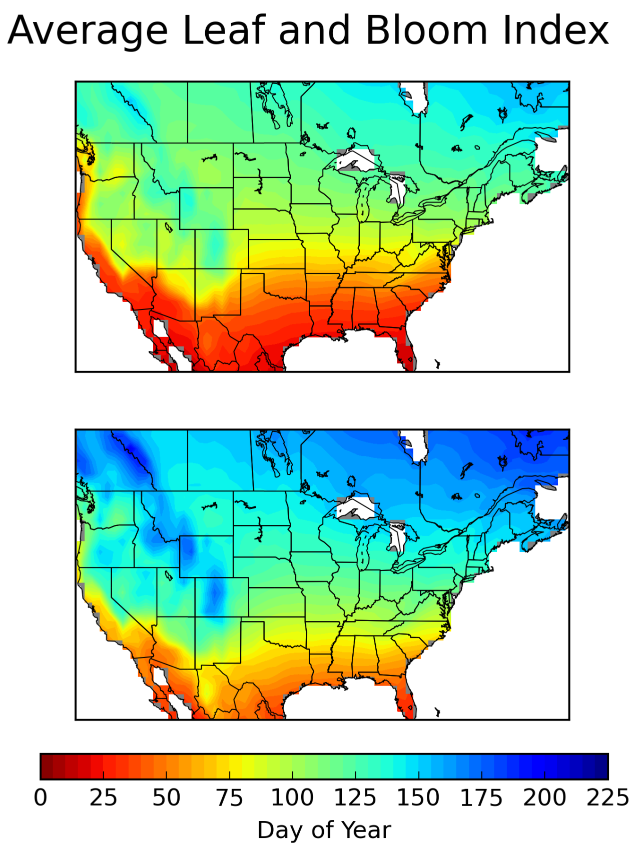

Figure 1: Average first leaf and bloom index composite maps using the BEST gridded data over the 1981-2010 climatological period. (Mueller, 2013).

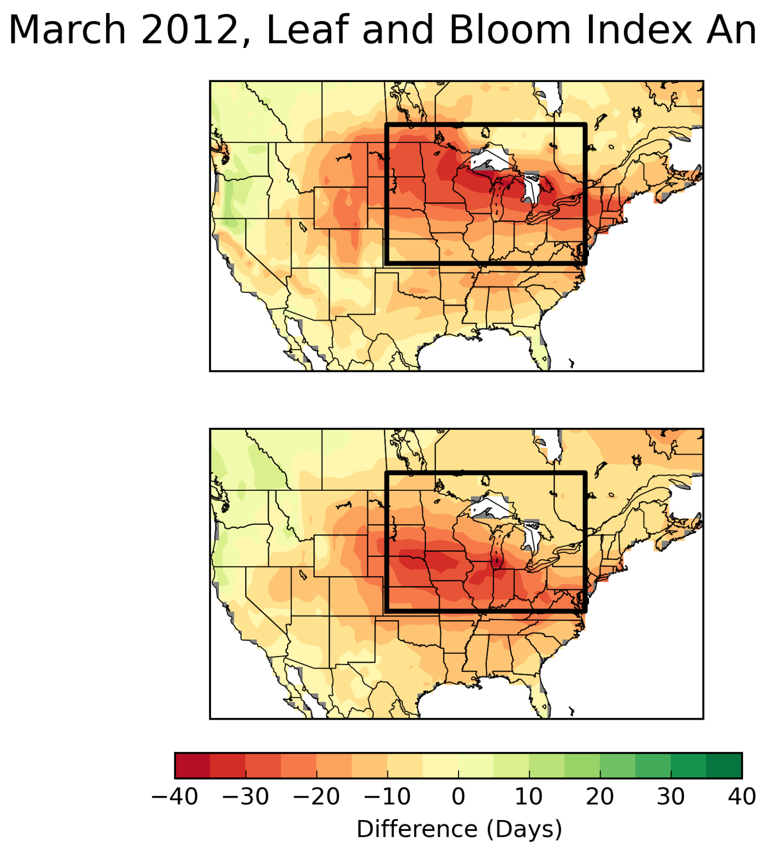

Figure 2: Using the the 2012 SI-x, leaf and bloom index anomalies are calculated in their difference from the climatological mean (1981-2010) in units of days. The outlined black box denotes the restricted geographic domain used in further calculations (37.5°N to 50.5°N and -101.5°W to -75.5°W).

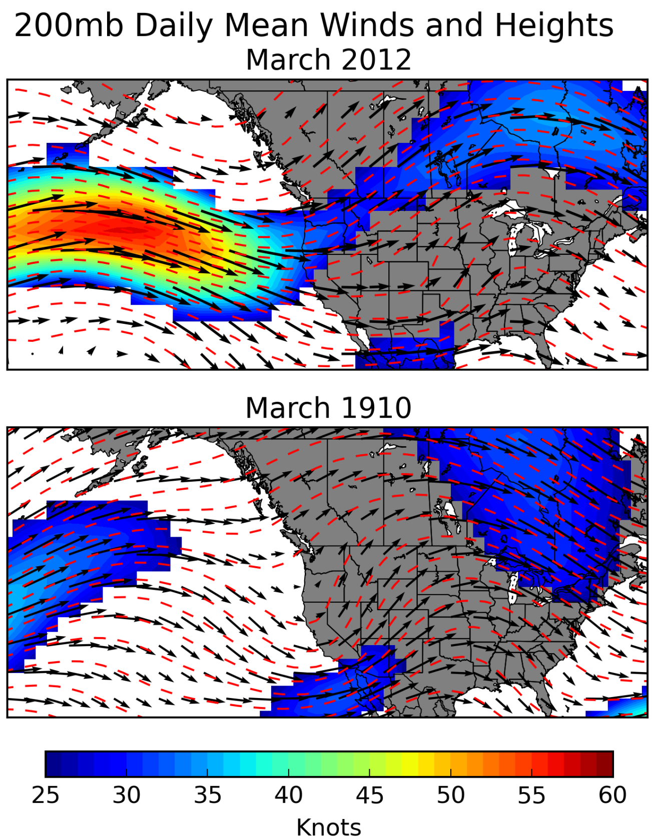

Figure 3: Mean 200mb heights (dashed contours) and u/v wind components (vectors) are plotted for peak warmth periods during March 12-23, 2012 and March 18-29, 1910 respectively as outlined in Dole et al. (2014). Winds in excess of 25 knots represent the filled-in color gradient. Maps are derived from NCEP-DOE Reanalysis II and NCEP-NCAR 20th Century Reanalysis projects (Kanamitsu et al., 2002; Compo et al., 2011)

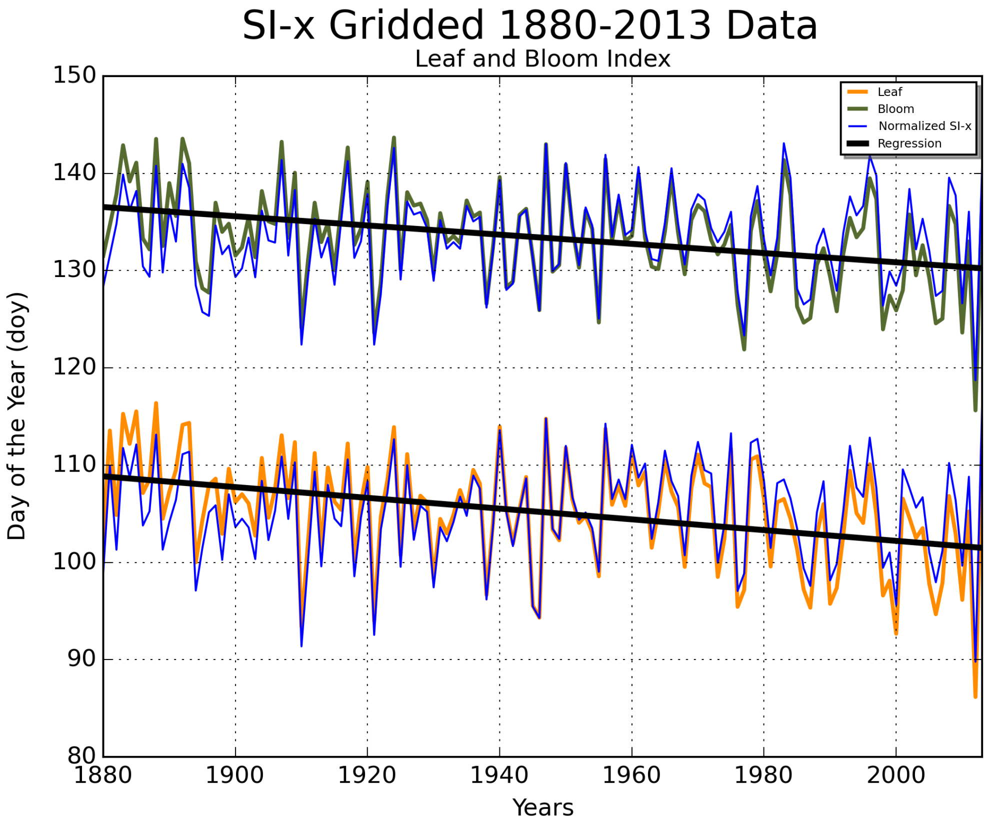

Figure 4: The same gridded indices as figures 1 and 2 are used to calculate the first leaf and bloom from 1880-2013. SI-x are further normalized by removing the linear trend over the period to later compute detrended z-scores. A simple least squares regression is additionally plotted to note the trend in earlier than normal spring onset over the post-industrialization era.

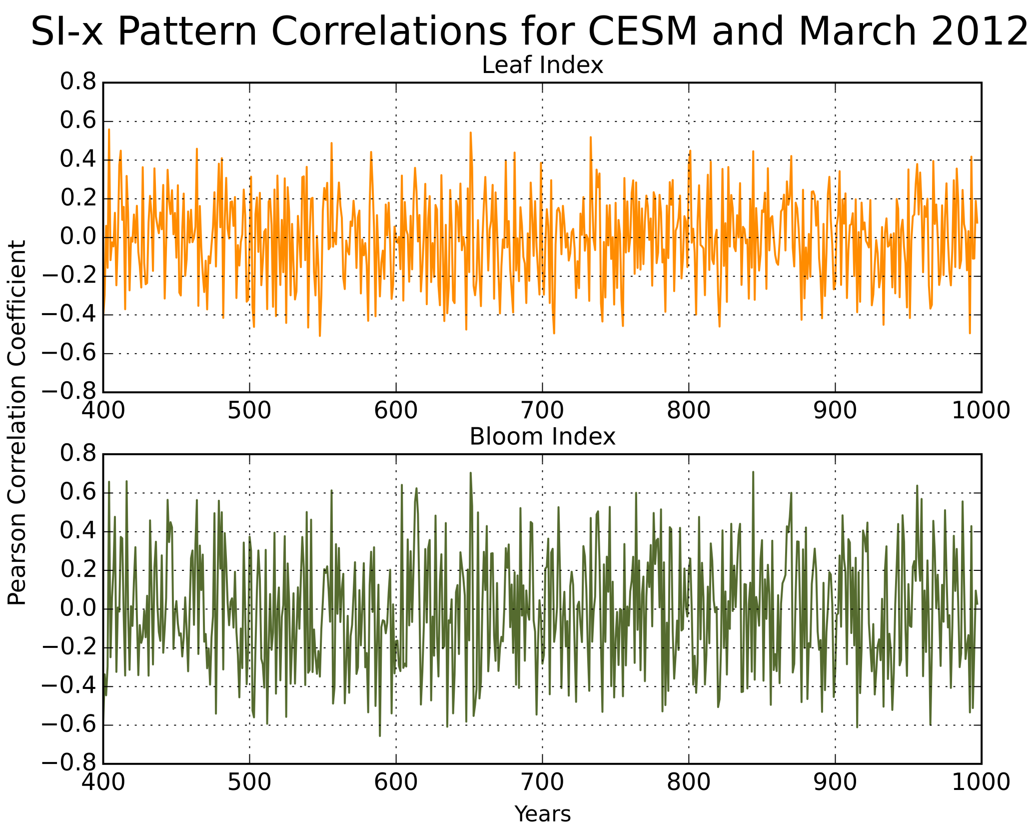

Figure 5: Pearson correlation coefficients are computed between 2012 leaf and bloom indices and the simulated pre-industrial CESM control run.

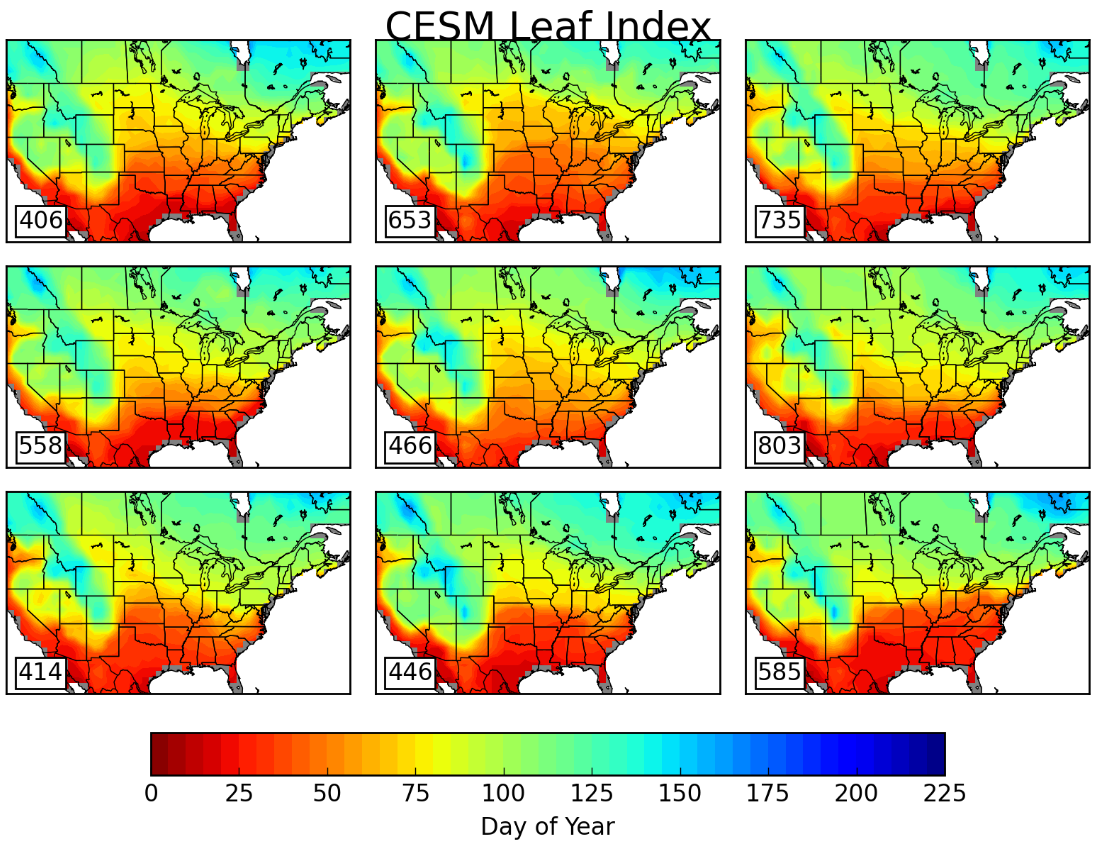

Figure 6: Nine closest correlations to 2012 first leaf index in the CESM control are estimated. Filled contours represent the day of the year beginning with January 1.

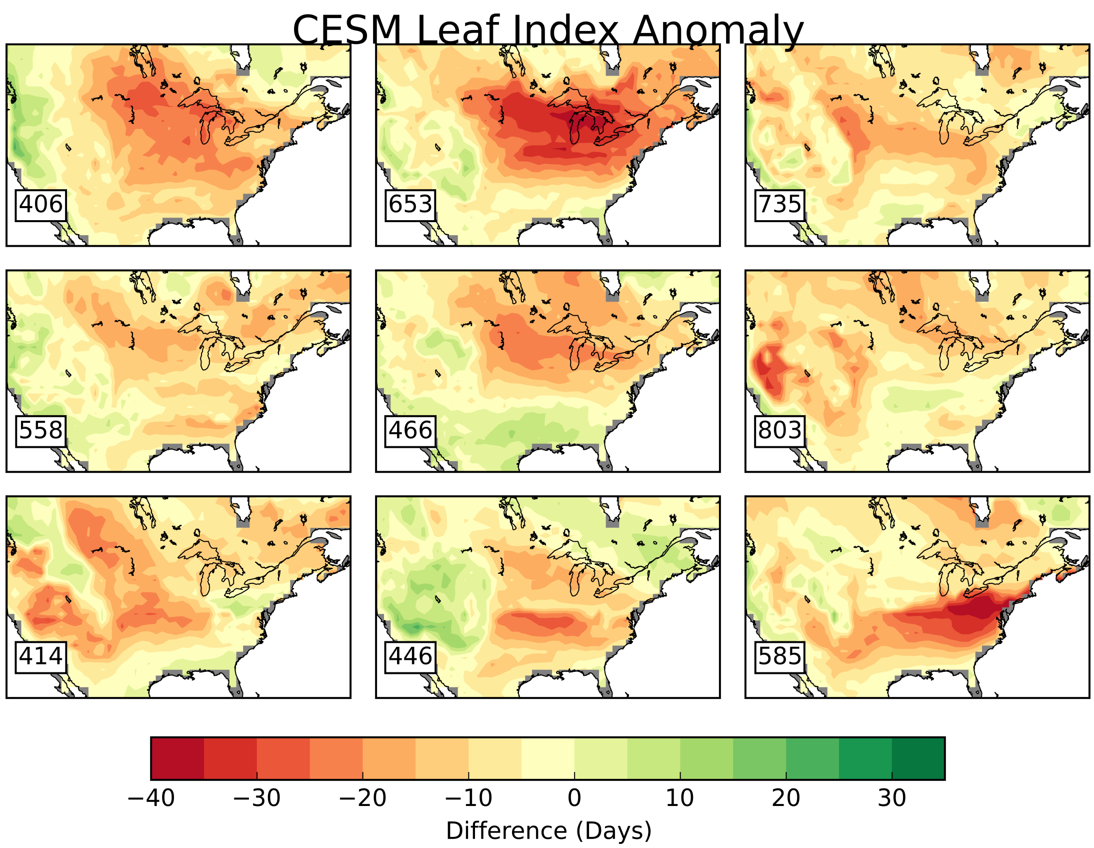

Figure 7: Same individual year matches as figure 4 are used to calculate the deviation from normal (days) utilizing the mean leaf index over the CESM control run from years 402-999.

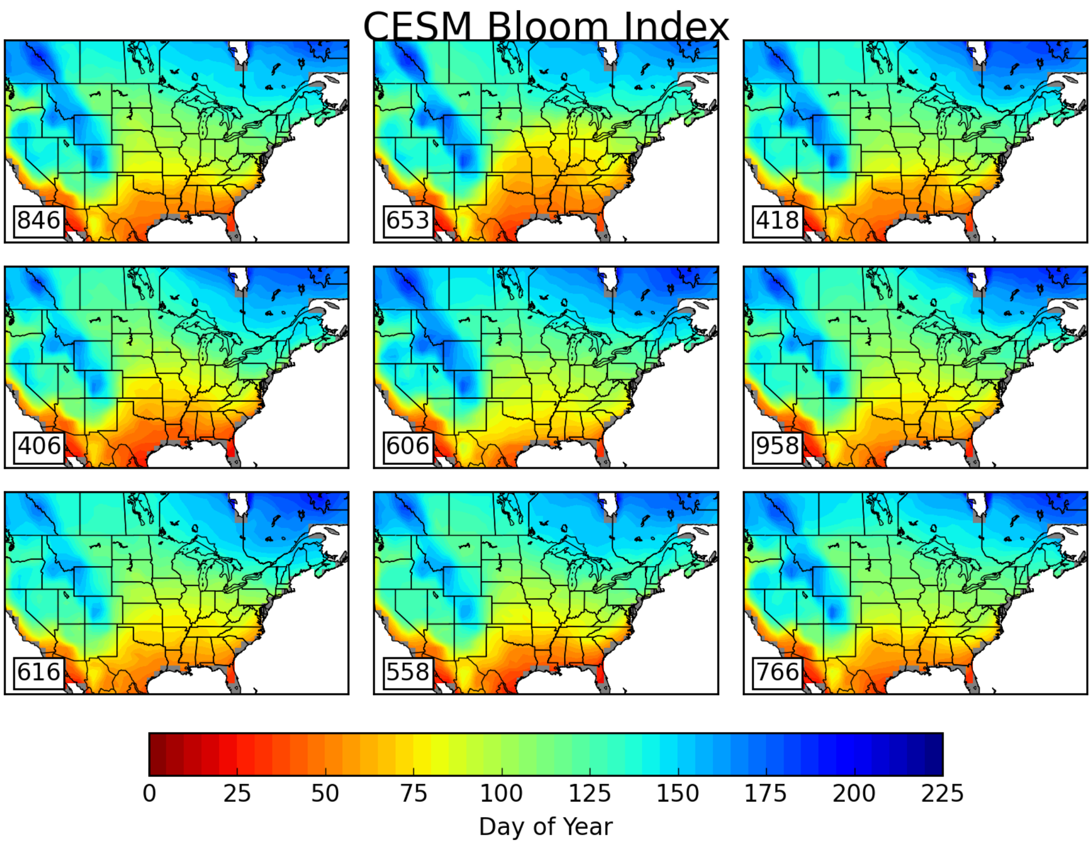

Figure 8: Nine closest correlations to 2012 first bloom index in the CESM control are estimated. Filled contours represent the day of the year beginning with January 1.

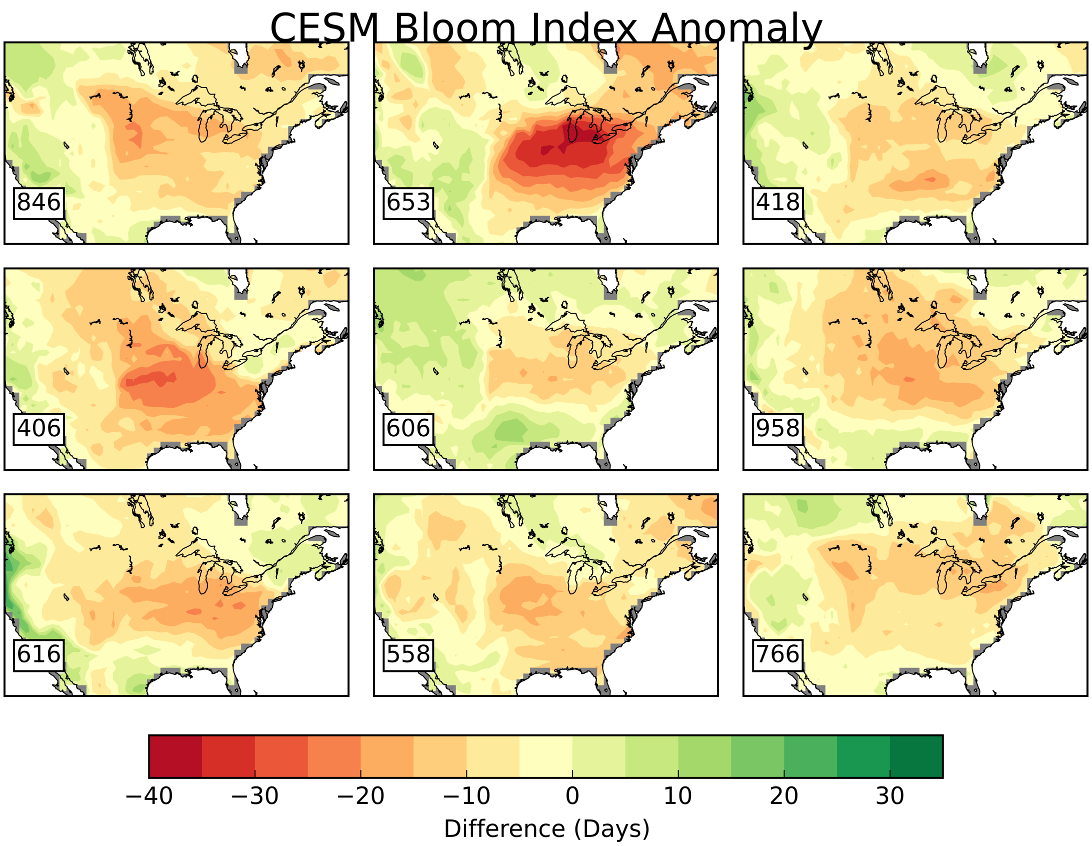

Figure 9: Same individual year matches as figure 6 are used to calculate the deviation from normal (days) utilizing the mean bloom index over the CESM control run from years 402-999.

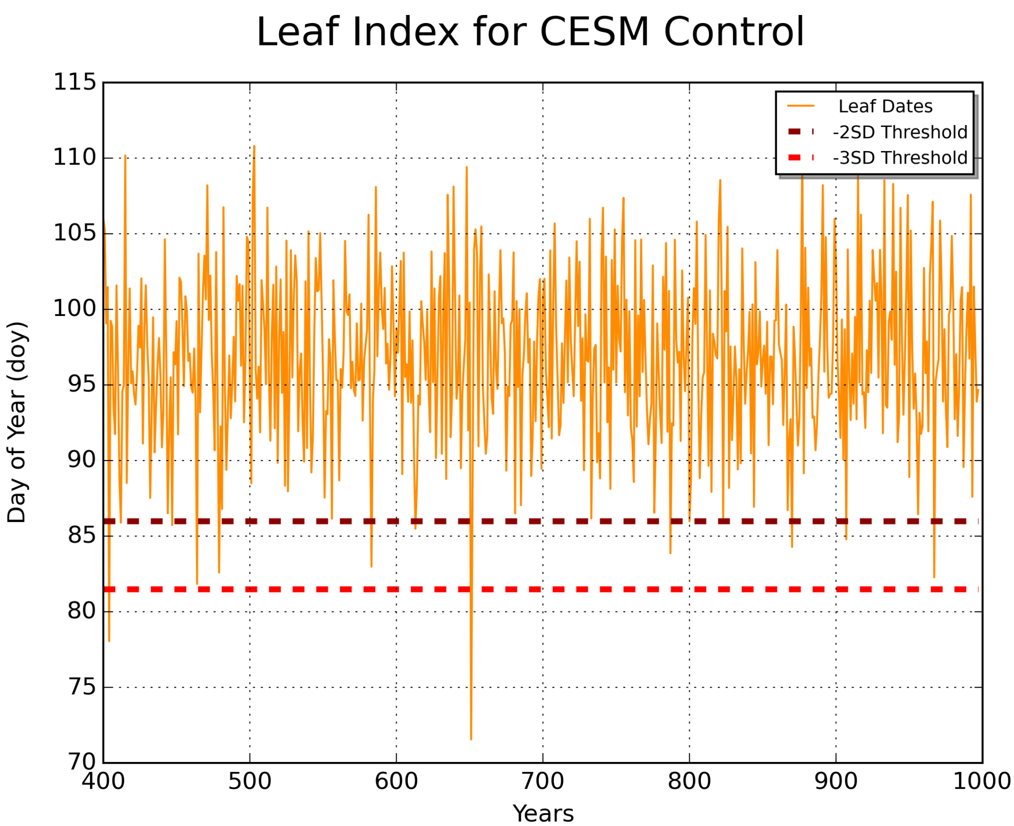

Figure 10: Time series of leaf indices computed over CESM control (years 402-999) against the normalized 2012 threshold of minus three standard deviations. Units again assume the day of the year beginning with January 1.

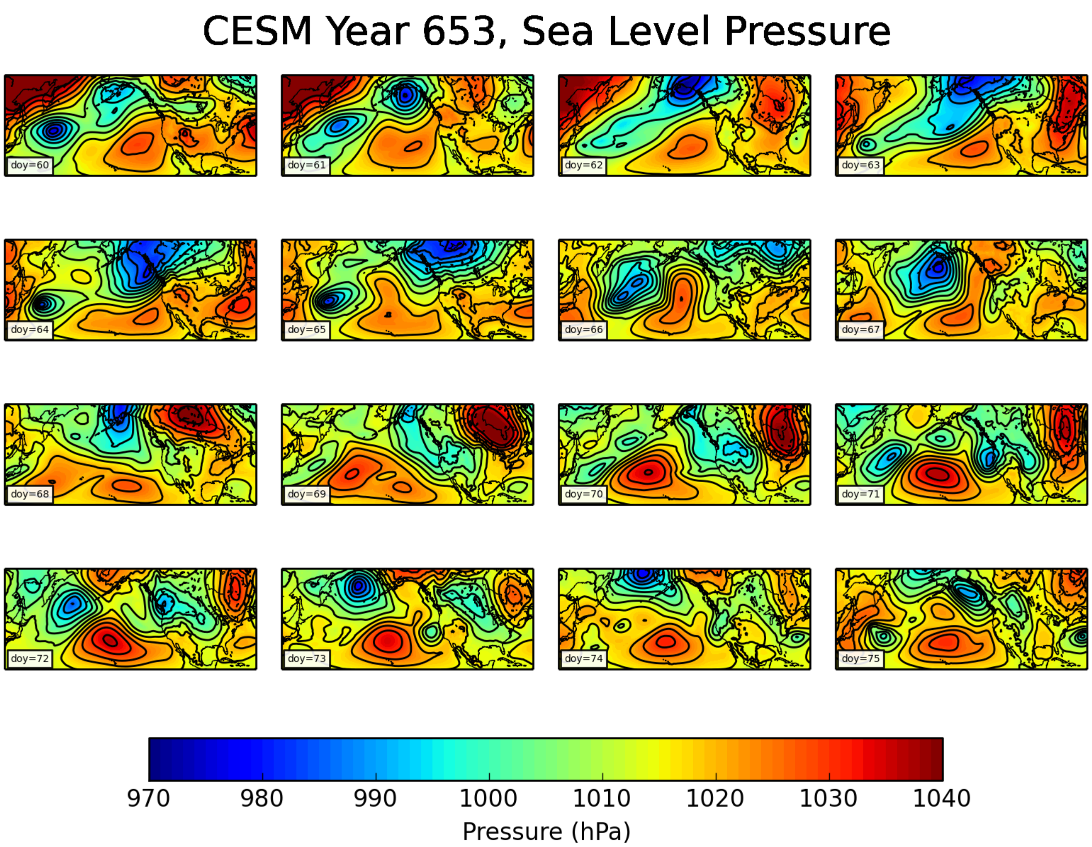

Figure 11: Sea level pressure is denoted by the filled contours for the period leading up to and during the early season warmth for Year 653 in the CESM control simulation.

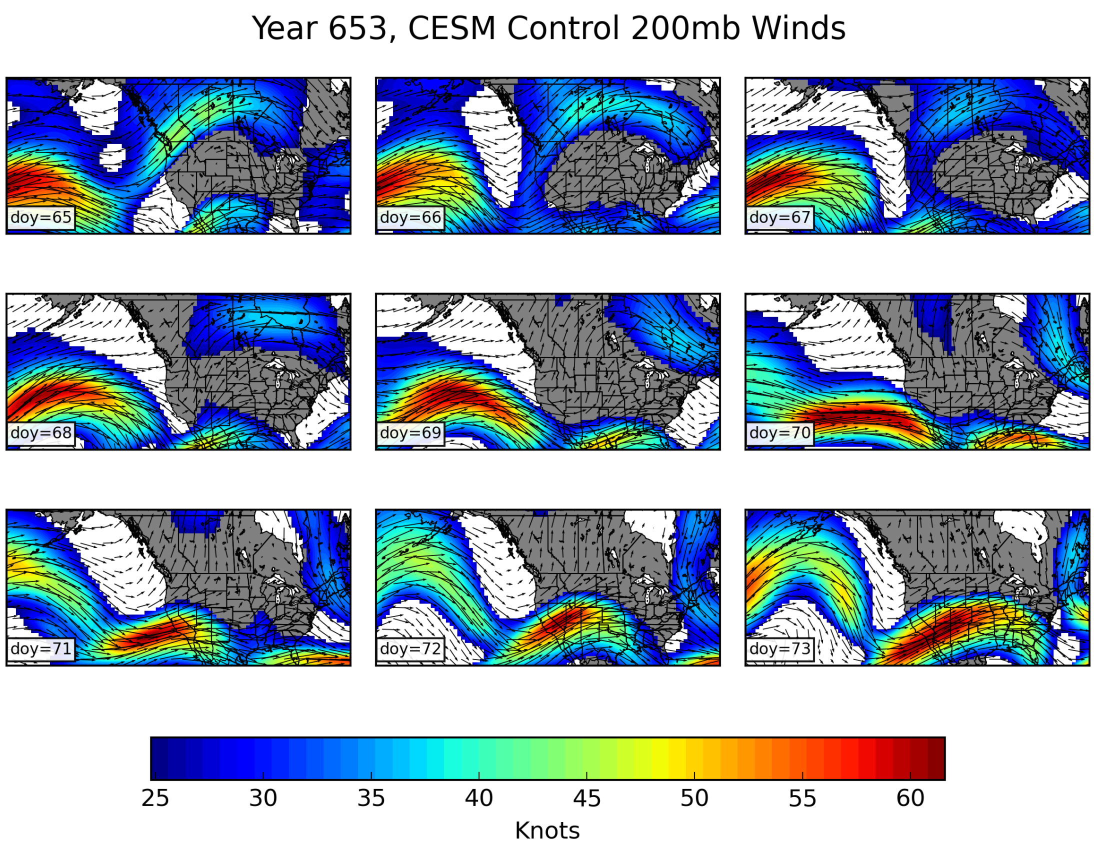

Figure 12: Wind quivers represent the u and v wind components at 200mb while filled contours highlight winds greater than 25 knots. The same time period is captured as the previous figure.

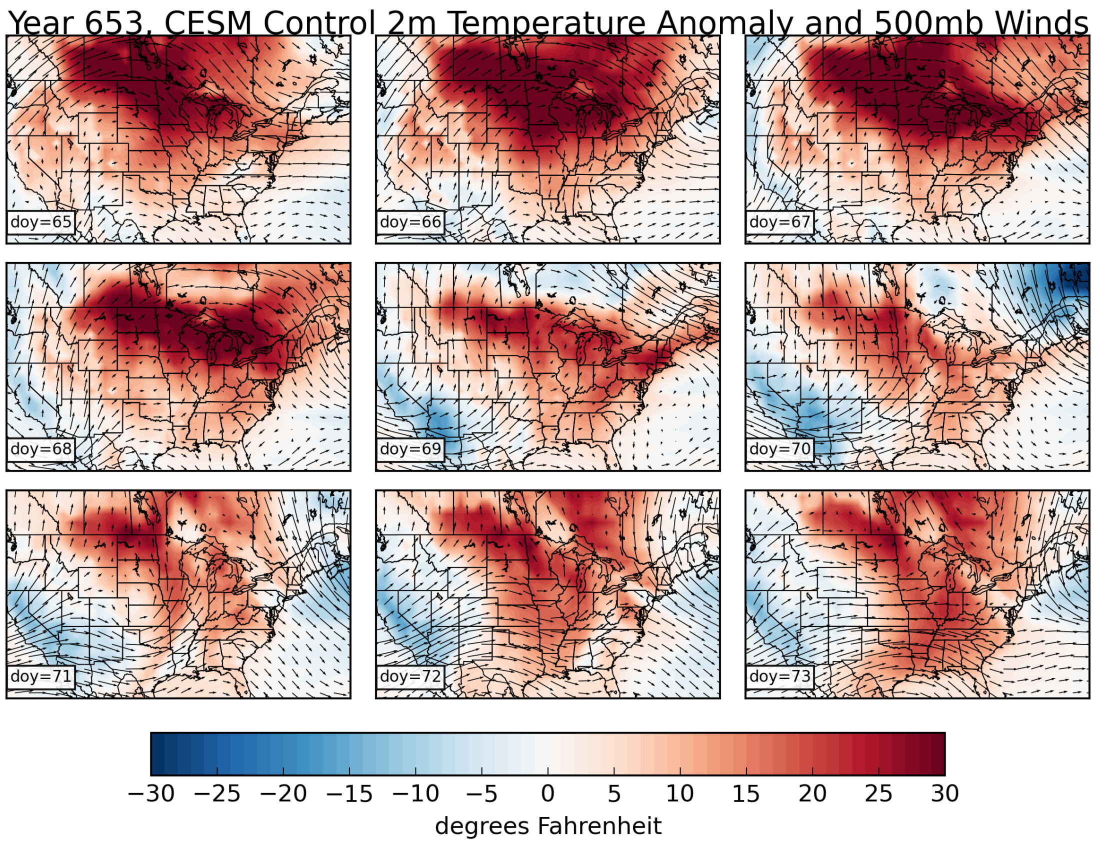

Figure 13: Filled contours represent the daily maximum temperature anomaly (°F) and vectors constitute the u and v wind components at 500mb. Daily maximum surface temperature climatologies were calculated over the 100-year period. The nine-day plot aligns with the greatest temperature anomalies and onset of spring for Year 653 in the CESM control run.

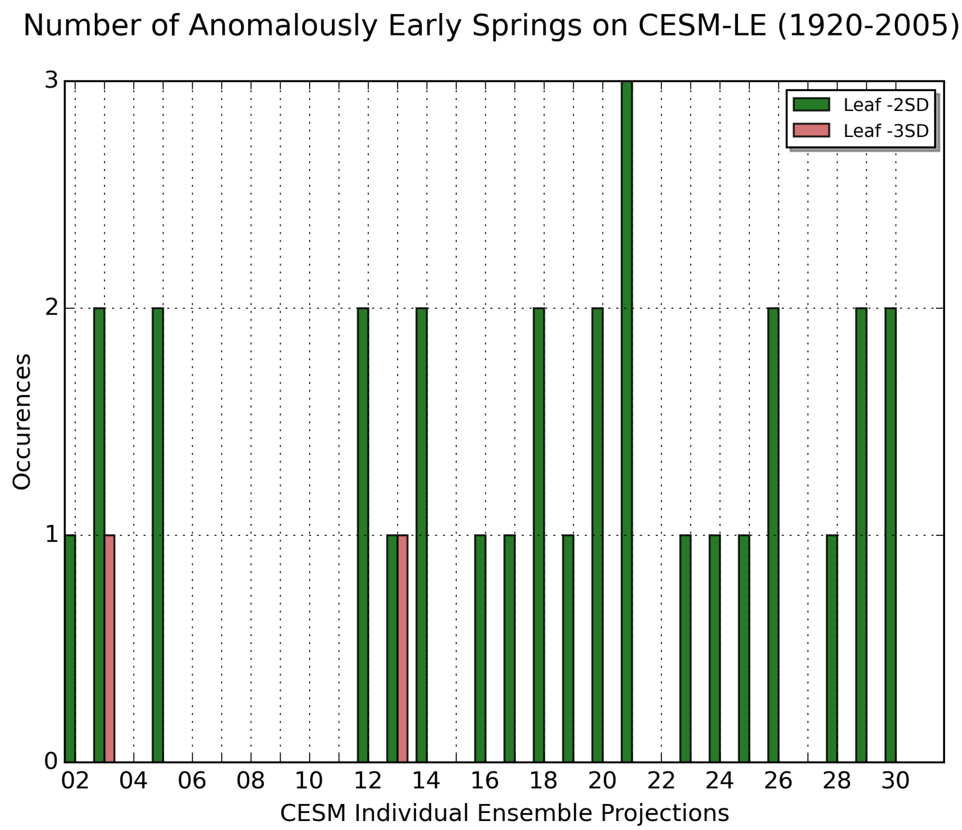

Figure 14: Occurrences of early springs are plotted for each of the thirty CESM large ensemble runs. Thresholds assume a minus two and minus three standard deviations. Each simulation assumes the same external forcing with small differences in initial conditions over 1920-2005 period (Kay et al., 2014).

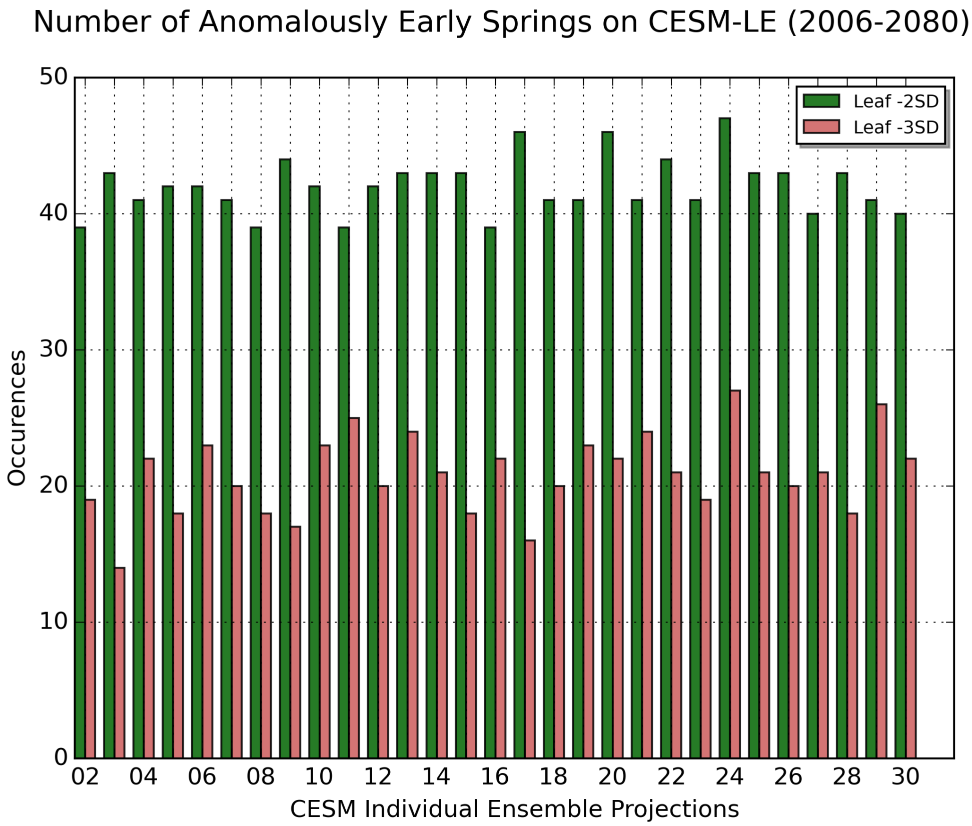

Figure 15: Frequency of early springs are highlighted for thirty future (2006-2080) RCP8.5 forced ensembles employing the same LENS project as the previous figure. Z-scores are calculated using the historical (1920-2005) leaf index and standard deviation as reference. Early spring thresholds are assembled for minus two and minus three standard deviations.